2008 11th IEEE International Conference on Computational Science and Engineering

A Novel Model for Combining Projection and Image Filtering using Kalman and Discrete Wavelet Transform in Computerized Tomography

Marcos A. M. Laia[1], Alexandre L. M. Levada[2], Leonardo C. Botega[1], Maurício F. L. Pereira[2], Paulo E. Cruvinel[3], Álvaro Macedo[3]

[1]*Federal University of São Carlos, Computer Departament, São Carlos SP, Brazil*

[2]*University of São Paulo, Physics Institute of São Carlos, São Carlos, SP, Brazil*

[3]*Brazilian Company of Agricultural Research, Embrapa Agricultural Instrumentation, São Carlos, SP, Brazil*

{marcos_laia, leonardo_botega}@dc.ufscar.br, alexandreluis@ursa.ifsc.usp.br, {cruvinel, alvaro}@cnpdia.embrapa.br, mauricioflp@if.sc.usp.br

Abstract

This paper presents a novel model for combining projection and image filtering in computerized tomography. First, it is used an a priori one-dimensional projection filtering, through an Extended Kalman Filter with Joint Estimation. Then, the reconstructed images, obtained filtered backprojection algorithms (including the use of Hamming windows), are filtered using the two-dimensional DWT and wavelet thresholding, a non-linear technique. Experiments considering only one filtering stage (a priori 1-D filtering or 2-D DWT image filtering) show images with significant higher noise levels and the combination showed great noise reduction. The obtained results lead to the conclusion that the proposed combining model is a valid and interesting tool for tomographic image analysis.

1. Introduction

Tomography consist in the action of light an object in many proportional directions and then store a set of obtained values that represents samples of projection. Each stored data is the mean of several inherent parameters of the beam light propagation path. The projections can be proceeding from several sources, like the X and γ-rays, magnetic resonance or ultra-sound. Based on the emitted intensity by the x-ray source and the captured intensity by the receptor located on the other extremity, the attenuation weight of the studied sample can be measured. This is a crucial data for the reconstruction process, making possible to hold a map of linear attenuation coefficients from the transversal plan of the object. This map is represented through pixels whose values are given by the CT numbers (computerized tomography). This numbers are normalized based on the water attenuation coefficient and defined by:

$$CT\ Number = \frac{\mu - \mu_{H_2O}}{\mu_{H_2O}} \times 1000 \qquad (1)$$

where μ is the attenuation coefficient of the analyzed body. With this number, it's possible to obtain an attenuation coefficient map, which allows a detailed analysis of the studied body. Using a reconstruction algorithm, it's possible to translate the coefficient attenuation map into a pixel representation and visualize the tomography as an image.

The reconstructive *x*-rays tomography had its first indicatives on the studies of Takahashi, whose study aimed to eliminate the undesirable plans, putting the *x*-ray source and the film on the same plan [22]. Oldendorf, in 1961, developed a rustical instrument to obtain images through the transmission of γ rays [20]. Later on, researchers as Hounsfield [8] and his team from EMI Corporation developed the first computerized tomographic scanner, commercially viable, dedicated to medical applications, and Cormack [2] formulated a coefficient matrix to sectional cuts, which could be obtained by the transmission of *x*-rays in many angles through a body.

1.1. CT and Soil Physics

Evaluating the evolution that has been occurring in the soil physics area, it is possible to notice the

978-0-7695-3193-9/08 $25.00 © 2008 IEEE
DOI 10.1109/CSE.2008.37

increasing interest of the scientific community to the development and application of non-invasive techniques for the study of soil characteristics. Amongst the used techniques, the *x*-ray computerized tomography excels in relation to others techniques, as gravimetrical and neutron probe [23], due to its precision in the extraction of physical attributes, as density and humidity [1, 3]. The main advantage offered by the computerized tomography is the possibility to use, after the reconstruction, image processing tools to assist the inquiry of the physical phenomena that occur in the soil, such as water and solute movement, formation of pores, textures and the distribution of roots. To evaluate these characteristics, a set of dedicated tomographic scanners was designed for application in soil physics in the last 20 years by the researchers of Embrapa Agricultural Instrumentation [4, 5, 12, 13, 18, 19]. Allied to the improvement of agricultural tomographic scanners, the development of filtering techniques came (surgiu) to improve the precision of the images, resulted from reconstruction algorithms, beyond the development of computational tools to assist the users in the information extraction [16, 17].

1.2. Noise

The term noise in tomographic images refers to a variation of the attenuation coefficients about the mean value when an image is obtained from a uniform object [26]. The image noise can be based on the standard deviation calculation and also on the power spectrum of the Wiener filter, which is visualized as a spatial frequency function, allowing the observation of the intensity and noise nature of the system, influencing the obtained image. The main source of noise in the TC images is the quantum mottle, defined as the statistical spatial and temporal variation on the photon number of the absorbed by the detector. Normally, reconstruction algorithms uses smooth filter to minimize the visual effect of this noise, together with some lost of spatial resolution. The electronic noise can have its origin in non-ideal electronic devices, such as non-pure resistors, non-ideal contact terminals, Joule effect and external interferences, independent from the signal (mechanical causes).

1.3. Objective

This study presents as objective, the application of an *a priori* filtering, using the Extended Kalman Filter with Joint Estimation and a non-linear bidimensional filter with the Wavelet Transform, applied over tomographic images of soil physics. The methods are described, implemented and combined in a novel model, for their results analysis.

2. Methodology

To obtain the data adopted in the experiments along this study, an X and γ ray tomographic scanner, from Embrapa Agricultural Instrumentation was used, making possible the composition of coefficient attenuation map with spatial resolution above 1mm [12, 13]. Hence, with the obtained projections, an Extended Kalman filtering with joint estimation was used, performing an *a Priori* filtering for noise reduction, based on predictions. The section 2.1 and 2.2 describe this process in details.

Later, the same 1-D projections used for the Kalman filtering are reconstructed using a Filtered BackProjection algorithm with and without Hamming Windows usage, producing filtered 2-D images. Thus, independent of the Kalman process, a non-linear filtering algorithm with Wavelet Transform was used. Taking use of the Haar basis (two coefficients), the algorithm divides the image into quadrants and then uses low-pass and high-pass functions, smoothing the image and preserving details and edges. The sections 2.4 and 2.5 describe these events.

As last approach, the two filtering methods are combined, making a novel model of tomographic image denoising. Following the same methodology as the independent approaches described in sections 2.2, 2.3, 2.4 and 2.5, the two methods are applied in sequence into the 1-D and 2-D data. The Figure 1 shows the schematic diagram of the proposed combining filtering model.

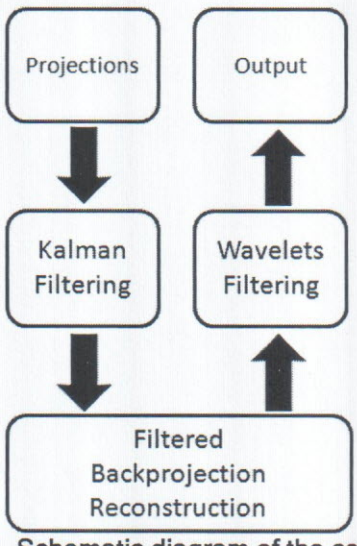

Figure 1. Schematic diagram of the combining filtering model

2.1. A Priori Projection Filtering

An *a priori* filtering allows projection noise separation before the tomographic projection reconstruction, with the objective of obtaining a best image quality. The tomographic projection is a discrete signal with its values based on the measurement of a photon, which crosses the soil samples e arrives at the receiver/counter. These samples are obtained with a constant energy in a determined time. The number of samples is dependent directly of the linear and angular steps, making a set of digital signals, eliminating the need of analogical-digital encoders usage. A digital filter characterizes itself by using one or a set of equations to treat digital signals, allowing the use of adaptative techniques, according to the signal, and other greater order filters [7].

2.2. Kalman Filter

Given a system with two equations, a process and a system equation (2, 3), where only the output can be observed, the discrete Kalman possess a way to estimate a process using feedbacks [25][11].

$$x_k = Fx_{k-1} + Bu_{k-1} + n_{k-1} \quad (2)$$

$$z_k = Hx_k + v_k \quad (3)$$

This filter estimates the process states in the time and, then, gets (noisy) measurements in a feedback. Then, the equations can be divided in two moments: time (4,5) and measurements update equations (6, 7, 8). The time update equations are responsible for the current estimation and error covariance of forward projections (in the time) to obtain the *a priori* estimation of the next time step. The measurement and correction update equations are responsible for feedback – in example, the incorporation of a new by measurement in *a priori* estimation to obtain an *a posteriori* estimation. The time update equations can be treated as prediction equations while the measurement equations can be treated as correction equations. Thus, the estimation algorithm joins a predictor-corrector algorithm to solve numerical problems as illustrates the Figure 2. It is possible to note that these equations project the time and covariance estimations through time in *k-1* step at *k* step.

$$K_k = P_k^- H^T (HP_k^- H^T + R)^{-1} \quad (4)$$

$$x_k = x_k^- + K_k(z_k - Hx_k^-) \quad (5)$$

$$P_k = (I - K_k H)P_k^- \quad (6)$$

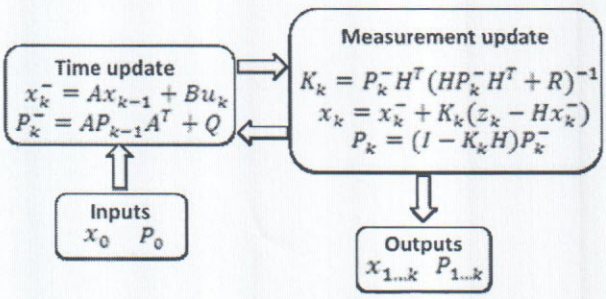

Figure 2. Discrete Kalman filter algorithm

$$x_k^- = Ax_{k-1} + Bu_k \quad (7)$$

$$P_k^- = AP_{k-1}A^T + Q \quad (8)$$

The first task in measurement update is to compute the Kalman gain (K_k). The next step is to update the measurement process and obtain z_k, generating an *a posteriori* estimated state (7). The final step is to obtain an error estimation covariance (8).
However, the process equation for tomography projections is affected for other non-Gaussian noises, as Poisson. Thus, the use of a filter for non-linear systems became itself necessary.

2.2.1. Extended Kalman Filter

A solution for non-linear systems is the extended Kalman filter [10]. Analyzing the Kalman filter prediction function is possible to observe that the filter behaves in linear form. The use of non-linear function can obtain an optimal prediction for next states, characterizing the extended Kalman filter. This algorithm applies the Kalman filter for non-linear system, linearizing all non-linear models and then the discrete filter equation can be applied. The non-linear system can be written in the form:

$$x_k = f(x_{k-1}, u_{k-1}, n_{k-1}) \quad (9)$$

$$z_k = h(x_k, v_k) \quad (10)$$

The algorithm can be adapted to solve non linear problems, as illustrates Figure 3. For the variance propagation, the Jacobians states or the Hessians matrices of the transition and observation functions must be known.

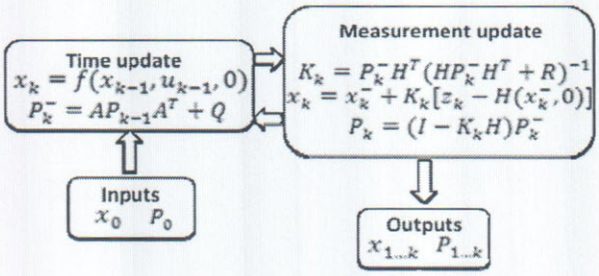

Figure 3. Extended Kalman Filter

2.2.2. Joint Estimation

The main problem is when the states and parameters functions must be identified. The prediction equations are described as:

$$x_k = f(x_{k-1}, n_{k-1}) \quad (11)$$

$$z_k = h(x_k, v_k) \quad (12)$$

The parameters estimation involves the non linear mapping determination as:

$$y_k = G(x_k, W_k) \quad (13)$$

where x_k is the input, W_k is the weight and y_k is the output, while G is parameterized by vector W_k. The non linear mapping can be made by an artificial neural network, where W is the weight. The learning process corresponds to the W parameters estimation. The training can be made with the samples pairs, which consists in a know input and a desire output $\{x_k, d_k\}$. The machine learning errors are defined by equation (14). The learning objective is to minimize the expected squared error:

$$e_k = d_k - G(x_k, W_k) \quad (14)$$

Using a model for neural network training, the extended Kalman filter can be used for parameter estimation, writing a new state-spatial representation [21]:

$$w_k = w_{k-1} + v_k \quad (15)$$

$$y_k = G(x_k, w_k) + e_k \quad (16)$$

where the w parameter corresponds to a stationary process with a identity state transition matrix, which was governed by process noise v (the variance chose determines the filtering performance). The output y corresponds of a non-linear observation of w. The extended Kalman filter can be applied directly, as a second order technique for parameters correction.
The problem in question consists in work on no observed input x and require an union between states and parameters, needed to consider a dual estimation problem, considering the non-linear discrete-temporal system dynamic:

$$x_k = f(x_{k-1}, W_k, n_{k-1}) \quad (17)$$

$$z_k = h(x_k, v_k) \quad (18)$$

where both the system state x_k and the parameter W_k, for the dynamic system, must be estimated from noisy signal z_k. The dynamic system can be understood as a neural network, where W is the set of weights. Thus, applying these equations in the extended Kalman filter, it has a new function for estimation and observation [14]. A filter's simplified form often is used by the joint estimation, where there is a possibility of estimation from Hidden Markov Chains, where the neural network weights are unobserved e can be trained by Kalman filter itself. The new equations can be written as:

$$\begin{bmatrix} x_k \\ W \end{bmatrix} = \begin{bmatrix} f(x_{k-1}, W, v_{k-1}) \\ I * W \end{bmatrix} \quad (19)$$

$$z_k = h(x_k, n_k) \quad (20)$$

The linearization matrix can be defined by the jacobian's function f and the function h, as observation matrix occulting the weights. The neural network used in this work was a perceptron multilayer with 1-10-1 neurons with a sigmoidal and linear transfer functions.

2.3. Two-Dimensional Reconstruction

The reconstruction algorithm based on the backprojection of the tomographic projections has its base on both the Fourier sections theorem and Radon transform. This theory established that the Fourier transform of the projection of an image $g(x, y)$ taking the angle θ, is equivalent to a piece of the two-dimensional transformation of $g(x, y)$. In other words, the Fourier transform of $P_\theta(t)$ supplies the values of $G(\omega_1, \omega_2)$ over the line BB' as illustrated in Figure 4.
A way to facilitate the visualization of filtered backprojected reconstruction is to separate them in two

different equations. The first is to filter the projection data for each angle θ, as follows:

$$Q_\theta(t) = \int_{-\infty}^{\infty} S_\theta(\omega)|\omega| e^{j\omega t} d\omega \qquad (21)$$

where $S_\theta(\omega)$ represents the Fourier transform of the convoluted projections with a filter in a frequency domain. After, the filtered projections are back projected to obtain an object function, given by:

$$g(x,y) = \int_0^{\pi} Q_\theta(x\cos\theta + y\,sen\theta)\, d\theta \qquad (22)$$

where each component represents a pixel of coordinate (x,y) in the reconstructed image $g(x,y)$. In a distinguishing manner, the discrete filtered backprojection is represented by the (21):

$$\hat{\tilde{g}}(x,y) = \frac{\pi}{K}\sum_{i=1}^{K} Q_\theta(x\cos\theta_i + y\,sen\,\theta_i) \qquad (23)$$

where K angles θ_i are the discrete values of θ for each $P_\theta(t)$ known.

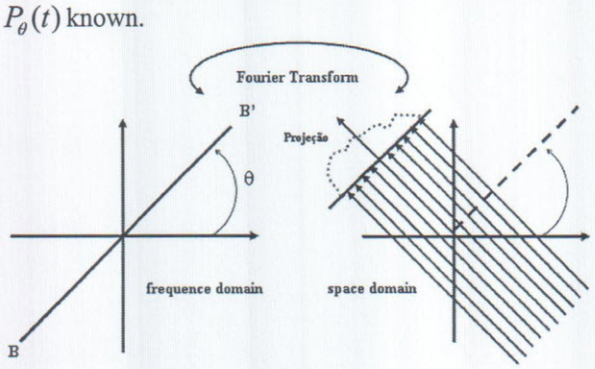

Figure 4. A schematic diagram for the Section Fourier Theorem

2.4. Two-Dimensional Filtering

The motivation for the inclusion of a two-dimensional filtering stage is the noise amplification caused by the filtered backprojection reconstruction technique, since the 1-D tomographic projections are filtered by a high pass filter, known as the Ram-Lak filter (a ramp filter). The presence of this filter is justified by the mathematical derivation of the filtered backprojection method. Thus, even these smooth 1-D projections, possibly with small amounts of noise, can generate noisy reconstructed images. Hence, we propose the use of the 2-D Discrete Wavelet Transform (DWT) in computerized tomography (CT) image filtering.

2.5. Wavelet Transform

One of the main advantages of the two-dimensional filtering, taking use of the Discrete Wavelet Transform, is that it preserves important image characteristics, by filtering smooth noisy areas, without much interference on edges and objects details presented on the image. This is possible by creating several well defined frequency subbands. In a wavelet decomposition, the image is decomposed in a set of subbands, which represent spatial oriented details at different scales [15]. The proposed methodology consists in, given a CT reconstructed image, convert it to the wavelet domain and perform noise reduction by wavelet thresholding.

2.5.1. The 2-D Discrete Wavelet Transform

The 2-D Discrete Wavelet Transform is a multiresolution representation of the original image data [24]. The DWT/IDWT is implemented by a *Perfect Reconstruction Filter Bank* (PRFB). The transformed signal is obtained by a sequence of low-pass/high-pass filtering stages followed by decimation operators, as shown in Figure 5.

Thus, the DWT can be completely characterized in terms of the analysis filters, defined by $h[]$, and its QMF pair (Quadrature Mirror Filter) $g[]$. Similarly, the IDWT is characterized in terms of the synthesis filters $\tilde{h}[]$ and $\tilde{g}[]$. Examples of wavelet filters are the Haar and Daubechies family [6].

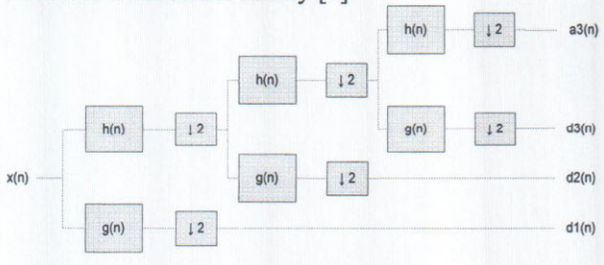

Figure 5. DWT decomposition by a filter bank

The 2-D separable DWT, also known as Square Wavelet Transform, is based on consecutive one-dimensional operations on columns and rows of the pixel matrix. The method first performs one step of the 1-D DWT on all rows, yielding a matrix where the left side contains down-sampled low-pass (h filter) coefficients of each row, and the right contains the high-pass (g filter) coefficients, as indicates Figure 6 [9]. Next, we apply one step to all columns, resulting in four types of coefficients:

1. *HH coefficients*: obtained by high-pass filtering in both directions (represent the diagonal features).

2. *HL coefficients*: obtained by high-pass filtering of the columns followed by low-pass filtering of the rows (represent the horizontal structures).

3. *LH coefficients*: obtained by low-pass filtering of the columns followed by high-pass filtering of the rows (represent the vertical structures).

4. *LL coefficients*: obtained by low-pass filtering in both directions and further processed on next levels (represent the approximation image).

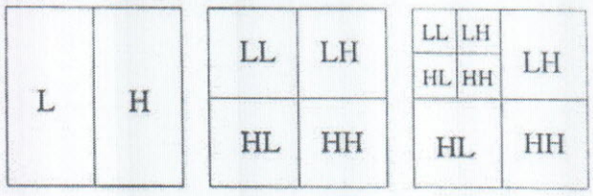

Figure 6. Illustration of a 2-D Wavelet Transform

2.5.2. Wavelet Thresholding

The analysis of a signal or image wavelet coefficients suggests that small coefficients are dominated by noise, while coefficients with a large absolute value carry more signal information. Thus, replacing the smallest, noisy coefficients by zero and applying the Inverse Wavelet Transform (IDWT) may lead to a reconstruction with the essential signal or image characteristics with less noise. More precisely, this idea is motivated by three assumptions [33]:

a.) The decorrelating property of a DWT creates a sparse signal, where most coefficients are zero or close to zero.
b.) Noise is spread out equally over all coefficients and the important signal singularities are still distinguishable from the noise coefficients.
c.) The noise level is not too high, so that we can recognize the signal wavelet coefficients.

In all experiments along this work, the wavelet thresholding was implemented by the suppression of the entire HH subband, since it concentrates the smallest coefficients (high frequency information).

3. Results

To test and evaluate the results of the presented model, the rehearsals were based in the study of two different samples, both ones provided from soil physics area, taking use of the tomographic scanner previously cited. In this work, all the experiments were executed in a Dual Core workstation with 2GB of memory. Both 2-D image reconstruction and *a posteriori* filtering via wavelet thresholding stages were implemented in C programming language. The Kalman filtering stage was built using the MATLAB environment.

First, it was adopted a sand sample acquired with 56 KeV under 10 seconds of exposure. Their results are shown in Figure 7, divided into: just reconstructed, Kalman filtering, Wavelet filtering and both. Later, the filtering algorithms were applied in a latosoil sample acquired with 58 KeV under 4 seconds of exposure, as shown in Figure 8, following the same arrangement.

4. Conclusions

In this paper, it was discussed the use of computerized tomography image filtering combining an *a priori* 1-D Kalman filtering and an *a posteriori* 2-D wavelet filtering. The contribution is to show that the combined approach can improve noise reduction in the final image.

The obtained results demonstrated that only an isolated filtering stage, by applying Hamming windows for example, would not be sufficient to completely noise removal, indicating that noise reduction on the computerized tomography acquired data can be further improved. A detailed interpretation of the obtained results in terms of noise removal, through visual inspection of a specialist, may be necessary to perform a correct analysis, since for each image or application there is an optimum trade-off between noise suppression and fine detail preservation. Future works may include a deeper analysis of noise removal effects on other type of images, such as medical data and the use of more complex wavelet thresholding techniques.

The original reconstructed images obtained only through the Filtered Backprojection algorithm are completely dominated by noise amplification. Even after the application of Hamming windows still shows significant levels of noise. The same behavior occurs for the images reconstructed using only 1-D projections Kalman filtering and images filtered with 2-D Wavelet filtering.

Finally, is possible to conclude that the filtering combination approach produced satisfactory noise reduction in the reconstructed images, leading to very different and interesting results. An important point, however, is to note that even the smoother reconstructed images preserve the relevant details, like edges and small inner structures. Thus, the possibility to combine a priori Kalman filtering, Hamming windows and a posteriori 2-D Wavelet filtering provided a very useful and valid model for computerized tomography image analysis.

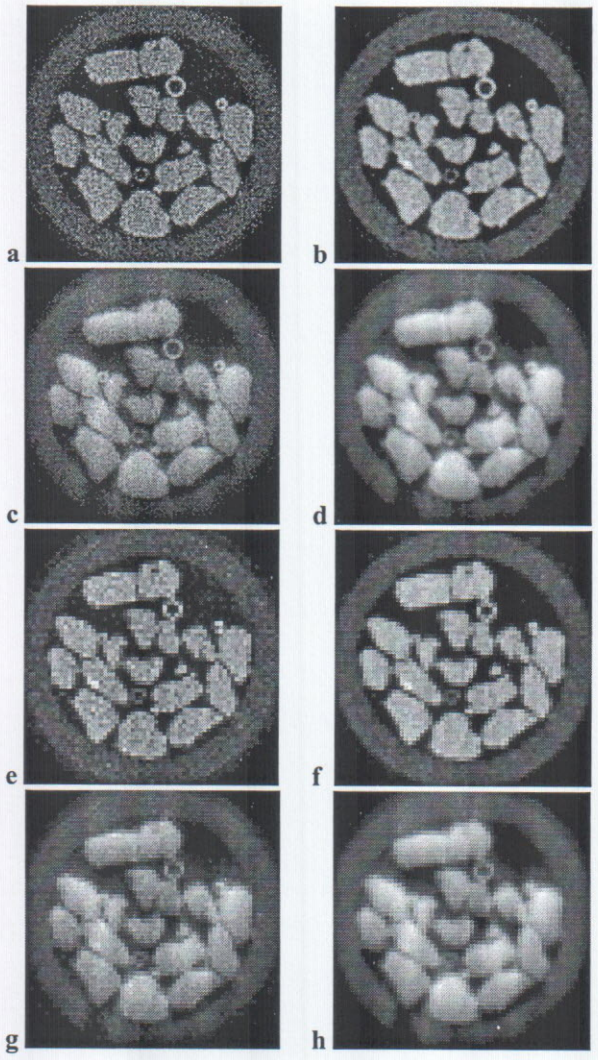

Figure 7. Filtering application over the sand sample: (a) Reconstructed image with Filtered Backprojection, (b) Reconstructed image using Backprojection with Hamming Window, (c) Extended Kalman filter, (d) Extended Kalman filer with Hamming Window, (e) Wavelet filtering with Haar basis, (f) Wavelet filtering with Haar basis and Hamming Window, (g) Extended Kalman filtering combined with Haar basis Wavelet, (h) Extended Kalman filtering combined with Haar basis Wavelet and Hamming Window.

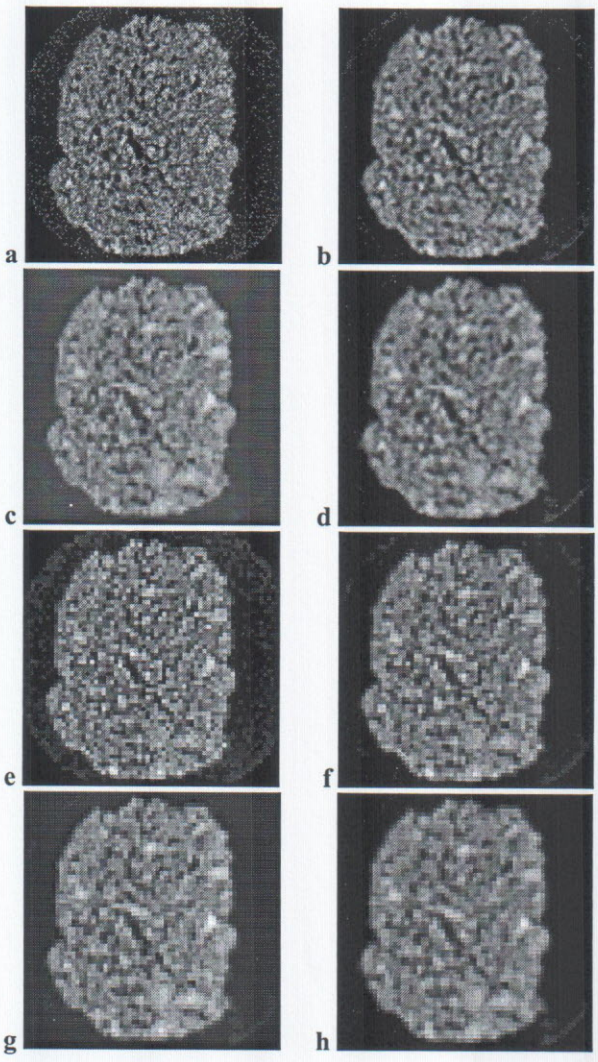

Figure 8. Filtering application over the latosoil sample: (a) Reconstructed image with Filtered Backprojection, (b) Reconstructed image using Backprojection with Hamming Window, (c) Extended Kalman filter, (d) Extended Kalman filer with Hamming Window, (e) Wavelet filtering with Haar basis, (f) Wavelet filtering with Haar basis and Hamming Window, (g) Extended Kalman filtering combined with Haar basis Wavelet, (h) Extended Kalman filtering combined with Haar basis Wavelet and Hamming Window.

5. References

[1] Aylmore, L. and Hainsworth, J. M. *The use of the computed assisted tomography to determine spatial distribution of soil water content. Australian .Journal Soil Res*, 21(4):435–443, 1983.

[2] Cormack, A.M. *Reconstruction of Densities from their Projections, with applications in Ratiological Physics.* Phys.Med.Biol, v.18, n.2, p. 195-207, (1973).

[3] Crestana, S. *A Tomografia Computadorizada com um novo método para estudos da física da água no solo.* Doutorado, Instituto de Física de São Carlos - Universidade de São Paulo, São Carlos, 1985.

[4] Cruvinel, P. E. *Minitomógrafo de Raios X e Raios computadorizado para aplicações multidisciplinares.* Doutorado, Universidade de Campinas, Campinas, 1987.

[5] Cruvinel, P. E., Cesareo, R., Crestana, S., and Mascarenhas, S. *X-and γ-rays computerized minitomograph scanner for soil science. IEEE - Transactions on Instrumentation and Measurement*, 39(5):745–750, 1990. IEEE.

[6] Daubechies, I. *Tem Lectures on Wavelets*, Philadelphia. SIAM, (1992).

[7] Haykin, S. *Adaptive Filter Theory*. Prentice-Hall, Inc, 3 edition,1996.

[8] Hounsfield, G.N. *Computadorized Transverse Axial Scanning (Tomography): Part I. Description of System.* British Journal of Radiology, n.46, p. 1016-1022, (1973)

[9] Jansen M., *Noise reduction by wavelet thresholding*, Springer-Verlag, New York, (2001).

[10] Julier,S. J. and Uhlmann, J. K. *A New Extension of the Kalman Filter to Nonlinear Systems.* In Proc. of AeroSense: The 11th Int. Symp. on *Aerospace/Defence Sensing, Simulation and Controls.*, 1997.

[11] Kalman, R.E. , *A new approach to Linear Filtering and Prediction Problems.* Research Institute for Advanced Study, Baltimore

[12] Macedo, Á. *Construção e uso de um tomógrafo com resolução micrométrica para aplicações em ciências do solo e do ambiente.* PhD thesis, Escola de Engenharia de São Carlos, São Carlos, 1997.

[13] Macedo, Á., Vaz, C., Pereira, J., Naime, J., Cruvinel, P., and Crestana, S. *Wood density determination by x- and gammaray tomography. International Journal of the Biology, Chemistry,Physics and Technology of Wood*, 56:535–540, 2002.

[14] Mathews, M. B. *A state-space approach to adaptive nonlinear filtering using recurrent neural networks.* In *Proceedings IASTED Internat. Symp. Artificial Intelligence Application and Neural Networks*, pages 197–200, 1990.

[15] Moulin, P. *Multiscale Image Decompositions and Wavelets, Handbook of Image and Video Processing*, Ed. Al Bovik, Sec. Ed., pp.347-359, 2005.

[16] Minatel, E. R. *Desenvolvimento de algoritmo para reconstrução e visualização tridimensional de imagens tomográficas com uso de técnicas freqüenciais e wavelets.* Master's thesis, Universidade Federal de São Carlos, Departamento de Computação, São Carlos - SP, 1997.

[17] Minatel, E. R. *Modelo computacional baseado em técnicasWavelets para relacionar imagens digitais obtidas em diferentes escalas e resoluções.* PhD thesis, Instituto de Física de São Carlos - Universidade de São Paulo, São Carlos, 2003

[18] Naime, J. M. *Projeto e construção de um minitomógrafoportátil para estudo de ciência de solo e plantas em campo.*Master's thesis, Escola de Engenharia de São Carlos – Universidade de São Paulo, São Carlos, 1994.

[19] Naime, J. M. *Um novo método para estudos dinâmicos, insitu, da infiltração da água na região não-saturada do solo.* PhD thesis, Escola de Engenharia de São Carlos, Universidade de São Paulo, São Carlos, SP, Brasil, 2001.

[20] Oldendorf, W.H. *Isolated Flying Spot Detection of Radiodensity Discontinuites – Dysplayng the Interhal Structural Pattern of a Complex Object*, IRE Transactions of Biomedical Eletronics, 8, p. 68-72, (1961).

[21] Singhal, S. and Wu, L. *Training multilayer perceptrons with the extended Kalman filter.* In *Advances in Neural Information ProcessingSystems 1*, pages 133–140, San Mateo, CA, 1989. Morgan Kauffman.

[22] Takahashi, H. et al. *Fluctuation in amplification of quanta with application to maser amplifiers.* J.Phy. Soc., Japan, vol.12, pp. 686-700, (1957).

[23] Teixeira, C. F. A., Moraes, S. O., and Simonete, M. A. *Desempenho do tensiômetro, tdr e sonda de nêutrons na determinação da umidade e condutividade hidráulica do solo. Revista Brasileira de Ciencia do Solo*, 29:161–168, 2005.

[24] Wei, D., Rajashekar, U., Bovik, A. C, *Wavelet Denoising for Image Enhancement, Handbook of Image and Video Processing*, Ed. Al Bovik, Sec. Ed., pp.157-165, 2005.

[25] Welch, G., and Bishop, G. *An Introduction to the Kalman Filter.* Chapel Hill: Departament of Computer Science, University of North Carolina, 2004

[26] Ziel, A. D., *Noise in measurements*- John Wiley & sons, inc.; 288p, 1976.